

EXPERIMENTAL STUDY OF UNSTEADY HEAT TRANSFER FROM A GAS-SUSPENSION FLOW IN THE INITIAL SECTION OF A CYLINDRICAL CHANNEL

A. V. Fafurin and K. R. Shangareev

UDC 536.24

Data are presented from experimental studies of unsteady heat transfer from a gas-suspension flow in a short cylindrical channel with an increase in the thermal load over time.

One feature of power-plant construction is the presence of axisymmetric channels enclosing a flow of heat-transfer agent. The gas flow here may contain solid particles which are not in dynamic or thermal equilibrium with the carrier phase. The concentration of particles in the flow may vary broadly. It was shown in [1, 2] that dispersion flows with a volume concentration of particles β , where

$$\beta = \frac{V_s}{V_s + V_0} \quad \text{or} \quad \beta = \frac{G_s}{G_0} \frac{\rho_0 w_0}{\rho_s w_s}, \quad (1)$$

and ranges from 0 to $3 \cdot 10^{-2}$, may be combined under the general term of gas suspension, and all of the laws governing these flows may be developed from common positions.

Units with short service periods, from fractions of a second to several minutes, are characterized by periods of increase, constancy, and decrease of the temperature of the heat-transfer agent, which corresponds to an increase, maintenance, and decrease of the thermal load. It is necessary to be able to reliably determine the heat-transfer coefficient under such conditions.

This article studies unsteady heat transfer from a gas-suspension flow in the initial section of a cylindrical channel, with an increase in thermal load. This situation corresponds to the time interval beginning with startup of the unit and ending with the beginning of its steady-state operation with respect to the temperature of the heat-transfer agent. The transient thermal conditions in the case we are studying are due to variations in the temperature of the heat-transfer agent and channel wall over time.

A constant increase in the temperature of the gas leads in turn to an additional increase in the temperature of the solid phase. The complexity of both the physical aspects of the flow and the mathematical aspects stems from the mutual effect of the phases on the thermal, thermodynamic, and kinematic characteristics of the system. This effect makes the system non-linear. In fact, the particle velocity deficit $\Delta w = w_0 - w_s$ is greater at the channel inlet than at the outlet. This means that the number Nu_s - the coefficient of heat transfer from the particles to the gas - will be higher at the beginning of the path of motion. This follows, in particular, from Drake's formula [2]:

$$Nu_s = 2 + 0.459 Re^{0.55} Pr^{0.33}; \quad Re = \frac{\rho_0 (w_0 - w_s) d_s}{\mu}. \quad (2)$$

The number Re decreases going away from the inlet, as does the number Nu_s . Other conditions being equal, this leads to a greater difference between the temperatures of the particles and the gas.

The presence of the gas temperature derivative has a complicated effect on particle subheating. An analysis done for the case $dT_0^*/dt = \text{const}$ shows that a positive value of the gas temperature derivative over time corresponds to greater subheating of the particles. The latter, located in the channel for a finite period of time, pass through several levels of

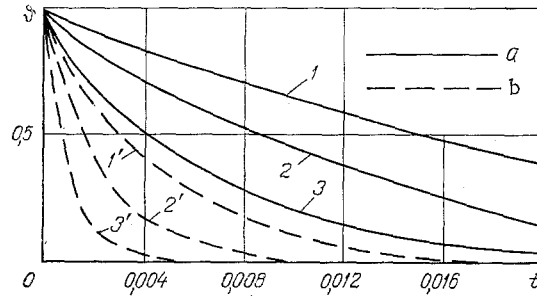


Fig. 1. Change in particle temperature over time (calculated from Eq. (6)): $\lambda_0 = 33.5 \cdot 10^{-3}$ W/mK; $c_s = 0.916$ kJ/kgK; a) Al_2O_3 , $\rho_s = 2700$ kg/m³; b) talc, $\rho_s = 500$ kg/m³; 1, 1') $d_s = 60$ μ m; 2, 2') 45; 3, 3') 30, t, sec.

gas temperature. All this further complicates the conditions of heat transfer, both from the gas to the particles and from the two-phase flow to the surface traversed by the flow.

The temperature deficit between the particles and gas ϑ can be found by solving the heat-transfer equation for the solid phase. For this, ignoring radiative energy transfer, we write the heat balance equation for the particles in the form

$$\frac{dT_s}{dt} = \frac{6\alpha_s}{\rho_s d_s c_s} (T_0 - T_s). \quad (3)$$

The solution of this equation may be represented as ($dT_0^*/dt = 0$)

$$T_{s(t)} = T_{s(0)} + \frac{q_s d_s}{Nu_s \lambda_0} \left[1 - \exp\left(-\frac{6Nu_s \lambda_0 t}{d_s^2 \rho_s c_s}\right) \right]. \quad (4)$$

It was considered in (4) that

$$q_s = \alpha_s (T_0 - T_s). \quad (5)$$

After some simple transformations of Eq. (4), we find that

$$\vartheta = 1 - \frac{T_{s(t)}}{T_0} = \left(1 - \frac{T_{s(0)}}{T_0}\right) \exp\left(-\frac{6Nu_s \lambda_0 t}{d_s^2 \rho_s c_s}\right). \quad (6)$$

Equation (6) permits calculation of the subheating of the particles with their passage along the gas channel. Figure 1 shows calculations performed for aluminum particles 30, 45, and 60 μ m in diameter and talc particles of the same size under the experimental conditions described above. It is apparent that the subheating depends significantly on particle size and density. An increase in these parameters is accompanied by an increase in subheating and leads to a change in the heat-transfer coefficient.

With an increase in thermal load, when the derivative of the gas-flow temperature over time is nontrivial, the solution of Eq. (3) has the form

$$T_0 - T_{s(t)} = \exp\left(-\frac{6Nu_s \lambda_0 t}{d_s^2 \rho_s c_s}\right) \left[\frac{q_s d_s}{Nu_s \lambda_0} + \int_{T_{0b}}^{T_{0e}} \exp\left(\frac{6Nu_s \lambda_0 t}{d_s^2 \rho_s c_s}\right) dT_0^* \right], \quad (7)$$

which reduces to forms (4) or (6) when $dT_0^*/dt = 0$.

We will assume constant dT_0^*/dt to evaluate the effect of the gas-temperature derivative on particle subheating. In this case, the integral of Eq. (7) can be represented as

$$\vartheta = \frac{T_0 - T_{s(t)}}{T_0 - T_{s(0)}} = \exp\left(-\frac{6Nu_s \lambda_0 t}{d_s^2 \rho_s c_s}\right) + \frac{d_s^2 \rho_s c_s t}{6Nu_s \lambda_0 (T_0 - T_{s(0)})} \frac{dT_0^*}{dt}. \quad (8)$$

Comparing Eqs. (6) and (8), we conclude that the temperature deficit ϑ is higher with an increase in thermal load ($dT_0^*/dt > 0$) — and lower with a decrease in same ($dT_0^*/dt < 0$) — than under steady-state conditions. This in turn leads to a relatively large deviation in the heat-transfer coefficient from its value under standard conditions. The second term of the right side of Eq. (8) is interesting in that it is proportional to the square of the diameter

of the particles. Obviously, its decrease will be accompanied by a decrease in the inertial properties of the particles and a drop in the particle temperature deficit. The heat-transfer coefficient is higher in unsteady two-phase flows than in steady two-phase flows.

An experimental study was made of unsteady heat transfer in a gas-suspension flow in a closed wind tunnel with a plasma-heated working fluid [3]. The test section was a cylindrical channel $\varnothing 45$ mm and a length of 10 diameters. Chromel-Alumel thermocouples with time constants no greater than 0.008 sec were installed on the 0.1-mm-thick outer surface of the tube at seven stations. Gas temperature was measured with a Chromel-Alumel thermocouple with a hot-junction diameter of 0.04 mm. Air flow rate was varied from 0.028 to 0.1 kg/sec and was held constant in each regime.

The solid phase used was alumina, with a particle diameter of 30 μm . Its consumption in all of the tests was a constant 0.0065 kg/sec. The particles were delivered by a nozzle installed in the prechamber 180 mm from the test-section inlet, the nozzle operating in conjunction with a disk feeder. The volume concentration of particles β did not exceed $5 \cdot 10^{-4}$. The velocity and temperature of the particles lagged behind the velocity and temperature of the gas flow at the test-section inlet.

The test data was analyzed by the method of local modeling [3]. As in the case of single-phase flows, the parameter of thermal transience

$$z_h = - \frac{\delta_h}{St} \frac{1}{\omega_0 \psi_h (h_0^* - h_w)} \frac{\partial (h_0^* - h_w)}{\partial t} \quad (9)$$

over time decreased, becoming roughly constant somewhat earlier than the gas temperature T_0^* did (Fig. 2). The enthalpy factor ψ_h decreased initially due to the rapid increase in gas temperature. This behavior lasted almost until the beginning of steady flow. The enthalpy factor then continuously increased, approaching unity.

Theoretical analysis shows that the sign of the thermal transience parameter determines whether the heat-transfer coefficient will deviate in the positive or negative direction relative to its steady-state value. In turn, the sign of z_h will depend on the sign of the derivative $[1/(T_0^* - T_w)] [d(T_0^* - T_w)/dt]$. Figure 2 shows the change in this quantity over time. Initially, the substantial change in T_0^* produces a substantial change in $(1/\Delta T) \cdot (d\Delta T/dt)$, with its absolute value decreasing. The derivative changes sign as the moment corresponding to $T_0^* = \text{const}$ is approached. However, the decrease in the derivative on the time section $T_0^* = \text{const}$ is insignificant and generally corresponds to evolution of the enthalpy factor.

The transience parameter z_h is more conservative over time (experimental values of z_h and St are shown for the fifth station of the test section). This is because the heat-transfer coefficient St nearly repeats the evolution of the derivative $(1/\Delta T) (d\Delta T/dt)$ and, since we have the following relation

$$z_h \sim \frac{1}{St} \frac{1}{\Delta T} \frac{d\Delta T}{dt}, \quad (10)$$

it is understood that a higher value of $(1/\Delta T) \cdot (d\Delta T/dt)$ corresponds to a higher value of heat-transfer coefficient.

The thermal transience parameter increases along the channel for a fixed moment of time despite a certain decrease in the enthalpy of the gas at the core of the flow and at the wall. The latter is connected with a decrease in the Stanton number and the enthalpy factor in the longitudinal coordinate function. This development is also associated with an increase in the thickness of the boundary layer. Such a pattern of change in z_h results in thermal transience having a greater effect on heat transfer.

Theoretical and experimental values of the heat-transfer coefficient in the transience parameter function were compared in [4]. Their satisfactory agreement was established. The effect of z_h when positive reaches 60% (up to $z_h = 10$) but is no greater than 20% when negative (down to $z_h = -10$).

Figure 3 shows data on heat transfer when $dT_0^*/dt > 0$ in the coordinates $St = f(\text{Re}_h^{**})$. As might be expected, the test data is located above the standard relation. This is indicative of the intensity of the heat transfer as a result of the effect of the factors of transience Ψ_{zh} , nonisothermality Ψ_h , and biphasality Ψ_{fh} , representing the ratio of the heat-transfer coefficient under the conditions being examined and standard conditions. The theoretical values of these functions were determined as follows.

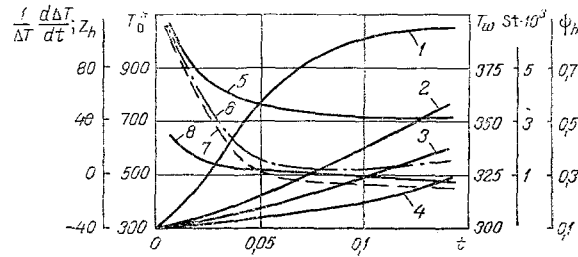


Fig. 2. Change in basic parameters of the flow (experiment): 1) T_0^* ; 2, 3, 4) T_w (for $x/D = 0.5$; 4.5; 7.5 respectively); 5) St ; 6) ψ_h ; 7) $(1/\Delta T)(d\Delta T/dt)$; 8) z_h . T_0^* , T_w , K.

In accordance with [5], the nonisothermality is equal to

$$\psi_h = 1 + \frac{4(1 - \sqrt{\Psi_h})}{\Psi_h(1 - 8.2 \sqrt{C_f \Psi_h})} \quad (11)$$

The heat-transfer law for these conditions can be realized numerically if the heat-flux distribution across the boundary layer is known. We will represent these heat fluxes in the form [6]

$$St = \sqrt{\frac{C_f}{2}} \int_{\xi_{1h}}^1 \sqrt{\rho/\rho_0} d\theta / \int_{\xi_{1h}}^1 \frac{\bar{q}}{q_0} \sqrt{\frac{\tau_0}{\tau}} \frac{d\xi_h}{\kappa \xi_h} \quad (12)$$

$$\bar{q}'_w = \left(\frac{\partial \bar{q}}{\partial \xi_h} \right)_{\xi_h \rightarrow 0} < 0; \quad \bar{q} = 1 + \bar{q}'_w \xi_h - (1 + \bar{q}'_w) \xi_h^d; \quad d = \frac{\bar{q}'_w}{1 + \bar{q}'_w}; \quad (13)$$

$$\bar{q}'_w > 0; \quad \bar{q} = 1 + \bar{q}'_w \xi_h - (2\bar{q}'_w + 3) \xi_h^2 + (2 + \bar{q}'_w) \xi_h^3, \quad (14)$$

where the heat-flux derivative is connected with the effect parameters by the expression

$$\left(\frac{\partial \bar{q}}{\partial \xi_h} \right)_{\xi_h \rightarrow 0} = \frac{1 - \psi_h}{\psi_h} \frac{q_s \delta_h}{q_w} - \frac{\delta_h}{St \omega_0 \psi_h (h_0^* - h_w)} \frac{\partial (h_0^* - h_w)}{\partial t} \quad (15)$$

The parameter of thermal biphasality (the first term on the right side of (15)) includes the quantity q_s , representing the amount of heat absorbed or released by the solid particles during their passage along the channel:

$$q_s = n S_s \alpha_s (T_s - T_0). \quad (16)$$

Representing the parameter of the two-phase nature of the heat by f_{sh} , and taking into account (16), from (15) we obtain

$$f_{sh} = \frac{\alpha_s \delta_h n S_s (T_s - T_0)}{q_w} \frac{1 - \psi_h}{\psi_h} \quad (17)$$

If the volume concentration of particles is β , their number per unit volume is n , and the volume and surface area of one particle are V and S_s , respectively, then the mass concentration of the particles G_s/G_0 equals

$$\frac{G_s}{G_0} = nV \frac{\rho_s}{\rho_0} \frac{w_s}{w_0} \quad (18)$$

For spherical particles, we have the equality

$$S = \frac{6V}{d_s} \quad (19)$$

Solving (17)-(19) simultaneously, we find

$$f_{sh} = \frac{G_s}{G_0} \frac{\rho_0 \omega_0}{\rho_s \omega_s} \frac{6\delta_h \alpha_s (T_s - T_0)}{q_w d_s} \frac{(1 - \psi_h)}{\psi_h} \quad (20)$$

Noting that $Nu_s = \alpha_s d_s / \lambda_0$, $Nu = St Pr Re$, from (20) we obtain

$$f_{sh} = \begin{cases} - \left[\frac{G_s}{G_0} \frac{\rho_0 \omega_0}{\rho_s \omega_s} \frac{6\delta_h D Nu_s}{d_s^2 \psi_h Nu} \left(\frac{T_s}{T_0} - 1 \right) \right], & -\psi_h < 1; \\ + \left[\frac{G_s}{G_0} \frac{\rho_0 \omega_0}{\rho_s \omega_s} \frac{6\delta_h D Nu_s}{d_s^2 \psi_h Nu} \left(\frac{T_s}{T_0} - 1 \right) \right], & +\psi_h > 1. \end{cases} \quad (21)$$

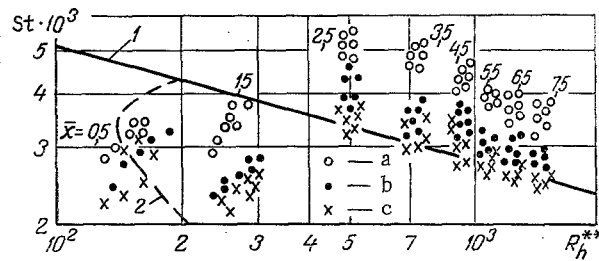


Fig. 3. Coefficient of heat transfer from gas-suspension flow: (a — St ; b — St/ψ_h ; c — $St/\psi_h\psi_{zh}\psi_{fh}$; $t = 0.01-0.12$ sec; $G_\Sigma = 0.042$ kg/sec; $G_S/G_\Sigma = 0.154$; $T_0^* = 300-800^\circ\text{K}$): 1) calculation with Eq. (22); 2) calculation for laminar and transitional regimes [8].

It is known that positive values of f_{sh} correspond to the case where the heat-transfer coefficient St is less than its standard analog and that the opposite case prevails with negative f_{sh} .

It follows from (21) that if the heat flux is directed from the wall to the gas ($\psi_h > 1$, $T_S/T_0 < 1$), then the parameter f_{sh} will be negative and $(St/St_0)_{Re_h^{**}} > 1$. Reversal of the direction of heat flow results in a complex pattern, the qualitative and quantitative aspects of which depend to a large degree on the thermal state of the particles at the channel inlet.

If the particles and gas are in thermal equilibrium at the inlet, i.e., if their temperatures are equal, then when $\psi_h < 1$ the heat-transfer coefficient will always be greater, regardless of the channel section being studied. If the particles are cooler at the inlet, then the heat-transfer coefficient on the section in which they are heated will be less than unity ($(St/St_0)_{Re_h^{**}} < 1$). The heat-transfer coefficient on the section where the temperature of the particles is the same as the gas temperature will be equal to the single-phase analog of the coefficient. As the hot particles travel into the zone where the gas is cooled, the heat-transfer coefficient will increase. This increase, meanwhile, will be greater, the more the ratio T_S/T_0 differs from unity.

The quantitative effect of each of the above-noted factors is different with respect to both time and position along the channel. Transience will initially make a large contribution, since the derivative of the gas temperature with respect to time will be large and the temperature itself low. Gas temperature will increase with time, however, and the gas-temperature gradient will decrease. The effect of the nonisothermality will thus increase. The increase in gas temperature is also accompanied by an increase in the subheating of the particles (given the same residence time in the channel), so the effect of biphasality on heat transfer becomes more pronounced.

Kinematic integral and thermal characteristics of the system were calculated from transient boundary-layer equations closed by the corresponding expressions for the friction and heat-transfer laws, the form parameter H ($H = \delta^*/\delta^{**}$), and the velocity and temperature deficits. The initial parameters for the calculations were borrowed from experiments. It was found that, for the conditions examined ($dT_0^*/dt > 0$), the effect of biphasality on the heat-transfer coefficient does not exceed 10% if the volume concentration of particles in the flow is low ($\beta \sim 5 \cdot 10^{-4}$).

Introduction of a function accounting for nonisothermality into the heat-transfer law makes it impossible to generalize empirical data relative to the standard relation, represented as

$$St_0 = \frac{0.0128}{Re_h^{**0.25} Pr^{0.75}} \quad (22)$$

Analysis shows that thermal transience is a more important factor here than thermal biphasality, since for the conditions of the experiment, the first (ψ_{zh}) has a value of 1.35 and the second (ψ_{fh}) has a value of 0.9.

Allowing for the above effects makes it possible to generalize the test data relative to the standard relation (Fig. 3), with the heat-transfer law itself represented in the form

$$St = St_0 \psi_h \psi_{zh} \psi_{fh} \quad (23)$$

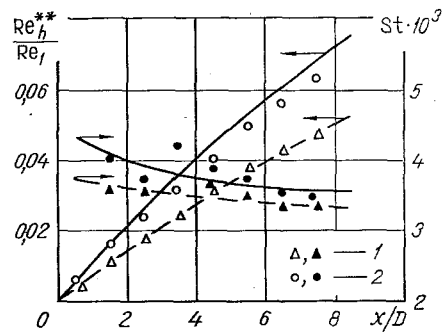


Fig. 4. Change in Reynolds number Re_h^{**} , normalized with respect to the analog Re_1 at the channel inlet, and the heat-transfer coefficient St as a function of the longitudinal coordinate (curves - calc. [6], points - expt.): 1) $dT_0^*/dt = 0$; $dT_w/dt = 230^\circ K/sec$; $T_0^* = 980^\circ K$; $G_\Sigma = 0.1028$ kg/sec; 2) $dT_0^*/dt = 13,500^\circ K/sec$; $dT_w/dt = 230^\circ K/sec$; $T_0^* = 734^\circ K$; $G_\Sigma = 0.1028$ kg/sec.

The deviation of the empirical data from the standard relation over the first two diameters is due to the following causes. The installation of a diffuser ahead of the test section ensures uniform velocity and temperature profiles at the section inlet. At the same time, it results in the particles in the initial diameters being concentrated on the channel axis. Thus, according to data obtained by the Institute of Theoretical and Applied Mechanics of the Siberian Branch of the Soviet Academy of Sciences, a uniform concentration of particles is achieved roughly in the second diameter. Together with this, it is known [7] that smooth entry into the first two diameters is associated with laminar and transitional flow, which leads to a decrease, followed by an increase, in wall temperature.

Figure 4 compares the results of calculations with transient energy and motion equations [6] against test data on the Reynolds number Re_h^{**} of the thermal boundary layer. It can be noted that this parameter continuously increases along the test section, the increase being more rapid, the greater the derivative dT_0^*/dt .

The heat-transfer coefficient St is inversely proportional to the criterion Re_h^{**} , with a lower value of Re_h^{**} corresponding to a higher Stanton number. However, the opposite pattern is seen in Fig. 4. This is explained by the presence of additional perturbing effects - transience and nonisothermality. In the first case, when $dT_0^*/dt = 0$, the effect of transience is of the order of 5%, and the effects of biphasality and nonisothermality are roughly 8% and 29%. In the second case, when $dT_0^*/dt \neq 0$, the respective effects of nonisothermality, biphasality, and transience are 23%, 10%, and 20-35%. This results in a higher heat-transfer coefficient. It should be noted that the error of this coefficient is 17%.

Comparison of the calculated thermal characteristics of the flow with the experimental values shows satisfactory agreement for both the number Re_h^{**} and the heat-transfer coefficient. All of the results are within the experimental error. The parameters characterizing biphasality ($\beta \sim 5 \cdot 10^{-4}$) do not have a substantial effect on the thermophysical characteristics of the flow, but they do permit a conclusion to be made regarding the direction of the effect of the solid phase on the relative heat-transfer coefficient. Thus, the effect of the disperse phase on the heat-transfer coefficient needs to be considered when $\beta \geq 3 \cdot 10^{-2}$ and with time derivatives of gas temperature up to $13,500^\circ K/sec$.

NOTATION

c , specific heat; C_f , friction coefficient; d_s , particle diameter; D , channel diameter; G , mass flow rate; h , enthalpy; Pr , Prandtl number; Re , Reynolds number; Re_h^{**} , Reynolds number of thermal boundary layer; St , Stanton number; T , temperature; t , time; q , heat flux; V , volume; w , velocity; x , longitudinal coordinate; $\bar{x} = x/D$, relative coordinate; α , heat-transfer coefficient; ρ , density; μ , absolute viscosity; λ , thermal conductivity; δ , boundary-layer thickness; ψ_h , enthalpy factor; Ψ , relative change in heat-transfer coefficient when $Re_h^{**} = \text{idem}$. Indices: 0, carrier phase (gas); s, solid phase; *, conditions with stagnation parameters; h, thermal; z, transience; w, wall.

LITERATURE CITED

1. Z. R. Gorbis, Heat Exchange and Hydrodynamics of Disperse Through Flows [in Russian], Énergiya, Moscow (1970).
2. S. Soy, Hydrodynamics of Multiphase Systems [Russian translation], Mir, Moscow (1971).
3. A. V. Fafurin, R. A. Muslimov, and K. R. Shangareev, "Experimental study of transient heat transfer in a two-phase flow on the initial section of a pipe," in: Heat and Mass Transfer in Chemical Engineering [in Russian], Kazan. Khim.-Tekhnol. Inst., Kazan (1978), pp. 52-55.
4. A. V. Fafurin, "Laws of friction and heat transfer in a turbulent boundary layer," in: Heat and Mass Transfer in Aircraft Engines [in Russian], Kazan Aviation Institute (1979), p. 62-69.
5. S. S. Kutateladze and A. I. Leont'ev, Heat and Mass Transfer and Friction in the Turbulent Boundary Layer [in Russian], Énergiya, Moscow (1972).
6. A. V. Fafurin, K. R. Shangareev, and R. A. Muslimov, "Transient heat transfer in a two-phase flow on the initial section of a pipe," in: Heat and Mass Transfer in Chemical Engineering [in Russian], Kazan. Khim.-Tekhnol. Inst. (1979), pp. 46-50.
7. P. N. Romanenko and I. V. Krylov, "Study of the effect of inlet conditions on heat transfer in the initial section of a pipe," Inzh.-Fiz. Zh., No. 4, 8-17 (1964).
8. E. U. Repik, "Experimental study of the structure of a turbulent boundary layer in the presence of a longitudinal pressure gradient," Tr. TsAGI, No. 1218, 19-35 (1970).

EXPERIMENTAL STUDY OF HEAT TRANSFER IN LIQUID BOILING IN HIGH-HEAT-CONDUCTIVITY CAPILLARY STRUCTURES

L. L. Vasil'ev, S. V. Konev,
P. Shtul'ts, and L. Khorvat

UDC 536.423:536.248.2

Results are presented from an experimental study of heat exchange in the boiling of water in copper capillary structures at low saturation vapor pressures.

The current intensive study of boiling processes stems from their heat-transfer coefficients and high maximum (critical) heat fluxes. The principal method of intensifying heat transfer is by using rough and capillary surfaces. For example, in the boiling of water on vapotron surfaces [1], the maximum heat flux reached 10^7 W/m². A value of $3 \cdot 10^7$ W/m² was achieved in heat removal on a capillary surface of the "inverted meniscus" type [2]. Among the shortcomings here, however, are large temperature gradients (vapotron) and small total heat flux (second case).

The most promising method of intensifying heat transfer is arranging for boiling in a capillary structure. The promise of this method owes to the achievement of high critical heat fluxes with small temperature gradients. Development of the method is currently proceeding in three directions: 1) boiling in submerged capillary structures [3]; 2) boiling in nonsubmerged capillary structures [4]; 3) boiling in a fluidized bed of dispersed particles [5]. Analysis of these procedures indicates that boiling in nonsubmerged capillary structures — so-called thin-film evaporators — is the most promising. The boiling mechanism in such evaporators depends significantly on the parameters of the capillary structure.

We investigated heat transfer in the boiling of water in nonsubmerged copper capillary structures, which are most effective at low saturation vapor pressures.

In examining heat transfer in boiling in capillary structures, we do not find an unequivocal answer to the question of the effect of the parameters of the structures on heat

A. V. Lykov Institute of Heat and Mass Transfer, Academy of Sciences of the Belorussian SSR, Minsk. State Research Institute of Machine Construction, Czechoslovak Socialist Republic. Translated from Inzhenerno-Fizicheskii Zhurnal, Vol. 42, No. 6, pp. 893-898, June, 1982. Original article submitted May 8, 1981.